Scientia Iranica A (2019) 26(4), 2286–2298

Sharif University of Technology
Scientia Iranica
Transactions A: Civil Engineering
http://scientiairanica.sharif.edu

Invited Paper

A novel damage detection method based on flexibility identification theory and data fusion technique

Y.Y. Cheng[a], C.Y. Zhao[a], and J. Zhang[a,b,*]

a. *School of Civil Engineering, Southeast University, Nanjing 210096, China.*
b. *Jiangsu Key Laboratory of Engineering Mechanics, Southeast University, Nanjing 210096, China.*

Received 31 March 2019; received in revised form 12 April 2019; accepted 13 May 2019

KEYWORDS
Damage detection;
Flexibility;
Dempster-Shafer evidence theory;
Noisy environment;
Curvature.

Abstract. An improved flexibility-based method is proposed in this study for damage detection. In this method, multi-scale convolution was utilized to decrease the interference of the measurement noise and the Dempster-Shafer evidence theory was adopted to combine all scale information to amplify the damage characteristics. Three main features distinguish the proposed method from the previous studies: 1) It is a kind of no-baseline flexibility-based method; that is, this method can locate the damage with the absence of intact structural flexibility serving as baseline; 2) Flexibility is estimated without requiring to know the structural mass, which is necessary in the traditional method for flexibility estimation; 3) By utilizing multi-scale space theory and data fusion approach, the proposed method has superior noise tolerance ability. Examples of both numerical and experimental types were studied to reveal the effectiveness and accuracy of the proposed method in different noise levels. Comparison between the traditional method and the proposed method demonstrated that the latter was quite suitable to detect damage to beams structure in a noisy environment.

1. Introduction

Vibration test is considered as a useful tool for performance evaluation of large-scale civil infrastructure to estimate structural modal parameters such as frequency, mode shapes, and flexibility [1-4]. Various damage detection methods have been developed based on these modal parameters and their derivatives [5-7]. Structural flexibility, defined as the displacement response of a structural node to a unit input force, has direct relationship with the variation of structural stiffness. It has attracted the interest of researchers especially in damage identification investigation. Zimmerman and Kaouk [8] first brought up a damage detection method based on the changes in the stiffness matrix, which was the inverse of flexibility. Lu et al. [9] recommended that flexibility curvature would be a good indicator for the detection of multiple damages. Grande and Imbimbo [10] proposed a fusion approach based on the flexibility for damage detection in structural applications in the case of multiple damage locations and three-dimensional systems. Zhang and Aktan [11] first used the Uniform Load Surface (ULS) to detect damage and defined the ULS as the flexibility matrix multiplied by the uniform force. Wang and Qiao [12] developed the ULS method by combining the Generalized Fractal Dimension (GFD) and Simplified Gapped-Smoothing (SGS) to detect different types of damage in composite beams. The flexibility-

*. *Corresponding author. Tel.: +86 15951934158;*
Fax: +86 025 52091355
E-mail addresses: chengyy@seu.edu.cn (Y.Y. Cheng); jian@seu.edu.cn (C.Y. Zhao); 220171151@seu.edu.cn (J. Zhang)

doi: 10.24200/sci.2019.21419

based damage detection methods reviewed above show good performance with numerical and experimental examples. However, these methods have one or two drawbacks, as described below, which greatly limit the development of flexibility-based damage detection method. Firstly, as we all know, the flexibility-based index is susceptible to measurement noise and the damage feature will be obscured by noise effect. Sometimes the method will fail to detect the changes if the damage is slight. Besides, most flexibility-based damage detection methods assume that not only structural mass but also intact structural flexibility is a prerequisite to flexibility identification [13-18]. However, in most cases, information of the intact structure is unavailable, especially for the structures with old ages, as no structural health monitoring data was recorded when they were built. Also, structural mass information has been recognized as an uncertainty source in structural identification.

To overcome the drawback of susceptibility to noise, several researchers have attempted to tackle this problem in curvature mode shapes from the perspective of optimal sampling interval [19] or signal processing [20,21], but no satisfactory result has been obtained. Cao et al. [22] suggested an improved curvature mode shape by integrating the Wavelet Transform (WT) and a Teager Energy Operator (TEO), called TEO-WT curvature mode shape, to detect damage. They used wavelet transform to filter noise and then, used Teager energy operator to amplify the local singularities of the signal. However, information of only one scale may not clearly reveal the local singularities of the signal; as the wavelet scale increases, the ability to reduce noise improves, but the capability of revealing local singularities of the signal is attenuated. With this consideration, fusing the multi-scale information provides the potential to identify damage in noisy conditions with high efficiency.

In recent years, information fusion techniques have attracted much attention in the field of structural damage detection and shown good performance in improving the efficiency of damage detection process. Guo [23] first proposed a structural damage detection method based on the information fusion technique. Two information sources were selected; one was the frequency data and the other was the mode shape. The results showed that with reference to a two-dimensional truss, damage detection based on the information fusion method worked better than that on the basis of a single information source, especially in the case of multiple damages. Based on the Dempster-Shafer evidence theory, Grande and Imbimbo [10,24] proposed a flexibility-based approach to detecting multiple damages by assuming the different mode shapes as primary sources. The results of case studies showed the ability and efficiency of the proposed approach in the case of multiple damages, limited number of identified parameters, and noise measurements. Guo and Xu [25] introduced a new hybrid method that utilized multi-scale space theory and data fusion approach to multiple damage detection in beams and plates.

In this study, based on the flexibility theory and information fusion technique, an improved ULS curvature method is proposed to improve the efficiency of damage detection in a noisy environment with no need to know the mass information and baseline data. The paper is organized as follows: in Section 2, the proposed method is illustrated. This section briefly reviews the identification method for flexibility with unknown mass and then, introduces the damage detection process using the Dempster-Shafer evidence theory. Section 3 validates effectiveness of the proposed method in contrast with the traditional ULS curvature method by utilizing a numerical example. In Section 4, an experimental example is conducted to verify the accuracy and efficiency of the proposed method. Finally, some conclusions are drawn in Section 5.

2. The proposed methodology

The proposed method is accomplished in two steps; in the first step, structural flexibility is estimated from impacting force and the corresponding accelerations by CMIF method without requiring to know the structural mass. In the second step, the Uniform Load Surface (ULS) is achieved based on the estimated flexibility and then, the ULS curve is selected as the input signal; multi-scale convolution with Gaussian kernel function is conducted to obtain the filtered ULS curvature. Dempster-Shafer evidence theory has been adopted to combine all scale information to amplify the damage characteristics and finally, obtain a reasonable result. The flowchart of the proposed method is illustrated in detail in Figure 1.

2.1. Flexibility identification with unknown mass

Various modal parameters identification methods have been studied to estimate structural flexibility, such as PolyMAX method [26], Complex Mode Indicator Function (CMIF) method [27], and Subspace Identification (SI) method [28]. In this work, CMIF method is employed to identify structural parameters and the process is briefly reviewed in the following. The displacement FRFs are first estimated from the recorded impact force and the corresponding accelerometer response. Then, Singular Value Decomposition (SVD) is applied to them:

$$\left[H^d(\omega)\right]_{N_0\times N_i} = \left[U(\omega)\right]_{N_0\times N_i}\left[S(\omega)\right]_{N_i\times N_i} \left[V(\omega)\right]^H_{N_i\times N_i}, \quad (1)$$

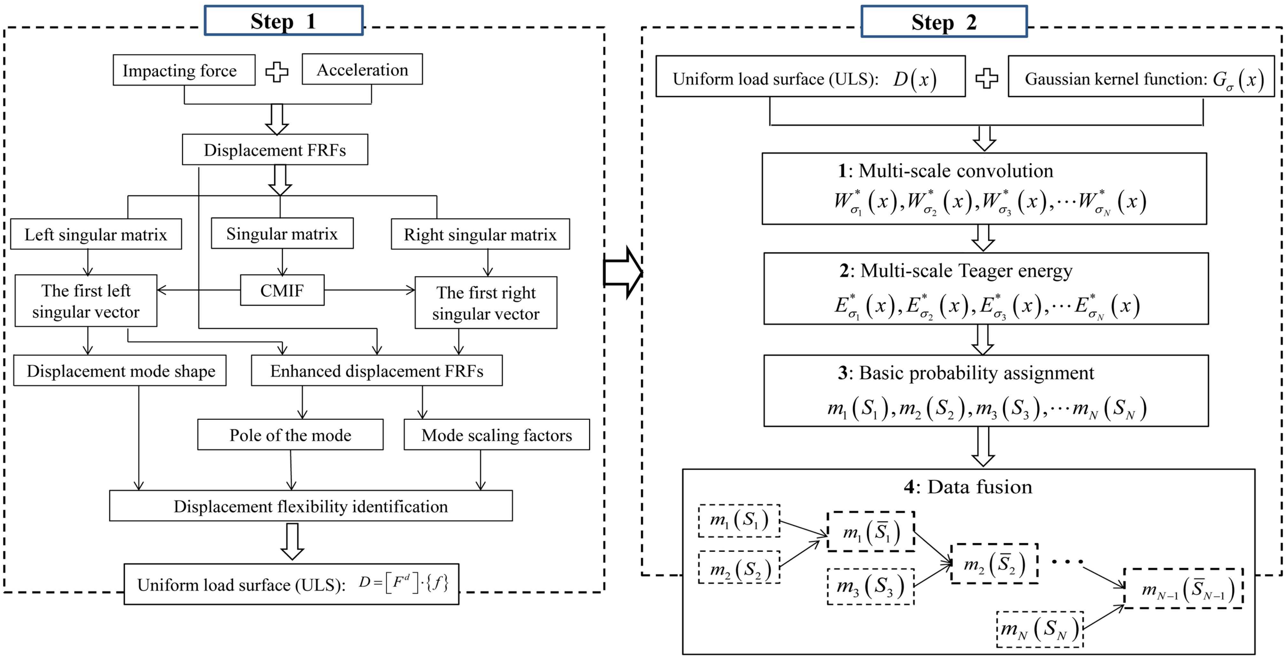

Figure 1. Framework of the proposed method.

where N_0 and N_i are the output number and input number, respectively; $[S(\omega)]$ is the singular value matrix; and $[U(\omega)]$ and $[V(\omega)]$ are the left and right singular vectors, respectively. It is known that the estimated displacement FRFs can also be rewritten in the form of modal expansion:

$$[H^d(\omega)]_{N_0\times N_i}=[\Phi]_{N_0\times 2N}\left[\frac{1}{j\omega-\lambda_r}\right]_{2N\times 2N}[L]^T_{2N\times N_i}, \quad (2)$$

where:

$$[\Phi]=\Big[\{\phi_1\},\cdots,\{\phi_r\},\cdots\{\phi_N\},\{\phi_1\}^*,\cdots,\{\phi_r\}^*,\cdots,\{\phi_N\}^*\Big].$$

$\{\phi_r\}$ is the rth mode shape and $\{\phi_r\}^*$ is the complex conjugate. $[L]$ is the modal participation matrix in which $L_r=Q_r\cdot\phi_{r,drv}$ for the rth mode, $\phi_{r,drv}$ is the mode shape vector of the driving point, and Q_r is the modal scaling factor. Eqs. (1) and (2) are essential to the same extent, but they are two different forms for displacement FRFs. The structural frequencies, damping ratios, and mode shapes can be identified from Eq. (1). The modal scaling factor can be solved by the least squares estimation formulation as follows:

$$\frac{1}{Q_r}=C_{1r}C_{2r}\begin{Bmatrix}eH(\omega_1)_r\\ eH(\omega_2)_r\\ \vdots\\ eH(\omega_k)_r\end{Bmatrix}^+\begin{Bmatrix}1/(j\omega_1-\lambda_r)\\ 1/(j\omega_2-\lambda_r)\\ \vdots\\ 1/(j\omega_k-\lambda_r)\end{Bmatrix}, \quad (3)$$

in which $C_{1r}=\{\phi_r\}^T\{\phi_r\}$, $C_{2r}=\{\phi_{r,drv}\}^T\{\phi_{r,drv}\}$, and $eH(\omega)_r=\{\phi_r\}^T[H^d(\omega)]\{\phi_{r,drv}\}^T$ represent the enhanced displacement FRFs. λ_r is the rth complex eigenvalue of the system.

Based on the identified modal parameters, the structural displacement FRFs can be estimated:

$$[H^d(\omega)]=\sum_{r=1}^{N}\left(\frac{Q_r\{\phi_r\}\{\phi_r\}^T}{j\omega-\lambda_r}+\frac{Q_r^*\{\phi_r^*\}\{\phi_r^*\}^T}{j\omega-\lambda_r^*}\right). \quad (4)$$

The flexibility matrix can be obtained when the displacement FRF is evaluated at $j\omega=0$:

$$[F^d]=\sum_{r=1}^{N}\left(\frac{Q_r\{\phi_r\}\{\phi_r\}^T}{-\lambda_r}+\frac{Q_r^*\{\phi_r^*\}\{\phi_r^*\}^T}{-\lambda_r^*}\right). \quad (5)$$

From the derivation procedure described above, it can be found that structural mass is unknown and thus, it is more practical in real civil engineering.

2.2. Damage detection based on ULS curvature change

Based on the identified structural flexibility, the Uniform Load Surface (ULS) values of the structure can be obtained by:

$$D=[F^d]\cdot\{f\}, \quad (6)$$

where $\{f\}$ is the uniform load. As we all know, structural damage is sensitivity to curvature of mode shape and thus, the ULS curvature change widely adopted as damage index is defined as follows:

$$ULS=|W_i-W_d|, \quad (7)$$

in which W_i and W_d denote the ULS curvatures for intact and damaged structures, respectively. The curvature is calculated by using the central differential equation:

$$W(x) = D_x'' = \frac{D_{x+1} - 2D_x + D_{x-1}}{l^2}, \tag{8}$$

where x is the number of structural nodes and l is the length of element. Effectiveness of the ULS curvature change has been verified by numerical and experimental examples in the literature. However, it can be seen that the intact structural flexibility is needed to serve as baseline in this method.

2.3. Damage detection based on improved ULS curvature

In addition to the necessity of the baseline data, the ULS curvature change has another noticeable drawback; it is susceptible to noise, which is caused by the second-order differentiation of ULS to obtain the curvature. This differentiation can amplify the slight noise present in the deflection and usually leads to a noise-dominated ULS curvature with obscured damage signature, especially in slight damages. Owing to the differential property of convolution, the following relationship holds:

$$f''(t) \otimes h(t) = f(t) \otimes h''(t), \tag{9}$$

where $f(t)$ and $h(t)$ are two arbitrary functions, $\otimes$ represents the convolution operation, and $f''(t)$ and $h''(t)$ represent the second-order derivatives of the two functions, respectively. As the second-order derivative of deflection is a curvature, we can use the second-order derivative of the Gaussian function to convolute ULS for substituting the convolution of ULS curvature with Gaussian kernel function. In this way, the operation of differentiation can be avoided and we can utilize the ULS directly to obtain the filtered ULS curvature by applying the second-order derivative to the Gaussian kernel function. That is:

$$W_\sigma^*(x) = G_\sigma(x) \otimes W(x) = G_\sigma(x) \otimes D''(x)$$
$$= G_\sigma''(x) \otimes D(x), \tag{10}$$

where W_σ^* represents the filtered ULS curvature under the scale σ and G_σ is the Gaussian kernel, which is generally expressed as:

$$G_\sigma(x) = \frac{1}{2\pi\sigma^2} e^{-\frac{x^2}{2\sigma^2}}. \tag{11}$$

The Gaussian kernel and its derivatives can usually be utilized as common smoothing kernels due to their linearity and shift invariance.

In order to enhance the singularity of the filtered ULS curvature, we conduct Teager Energy Operator (TEO) on the curvature, which was proposed by H.M. Teager and S.M. Teager [29] and Kaiser [30] used it to calculate the instantaneous energy of a temporal signal. It has the advantage of intensifying local singularities. For the point x, its TEO value can be calculated by the curvature value of this point and its neighbors:

$$E_\sigma(x) = (W_\sigma^*(x))^2 - W_\sigma^*(x-1)\, W_\sigma^*(x+1), \tag{12}$$

where E_σ is the TEO value at scale σ; $x-1$ and $x+1$ represent two neighbor points of x.

When the scale σ increases, the resolution gradually decreases and the damage singularity will be smoothed; when the scale decreases, the resolution gradually increases and the noise will obscure the damage signature. Thus, the Teager energy indicator often fails to identify the damage location based on only one single scale. Multi-scale representation is a crucial tool for describing certain inherent properties of an unknown signal. By changing the scale parameter σ, the multi-scale space can be constructed. A hybrid procedure considering multi-scale information, based on Dempster-Shafter's theory, is studied here to improve the efficiency in damage detecting, especially in a strong noise environment.

Consider a finite set, θ, of mutually exclusive and exhaustive propositions [31]:

$$\theta = \{el_1; el_2; el_3; \cdots; el_N\}. \tag{13}$$

For the damage detection problems analyzed in this paper, $el_i\,(i = 1, 2, \cdots, N)$ represents the N nodes to be identified as damaged or not. The power set 2^θ is defined to include all the damage scenarios. According to the theory of evidence, the basic probability assignment, named mass function $m(S)$, in which S is any subset of 2^θ, is defined as the mapping of 2^θ onto the interval $[0, 1]$, that is:

$$m : 2^\theta \to [0, 1]. \tag{14}$$

It should satisfy the following conditions:

$$m(\phi) = 0; \sum m(S) = 1. \tag{15}$$

The Dempster-Shafter's theory considers all the basic probability assignments from different information sources to enhance the accuracy of the final result. For multiple information sources S_k $(k = 1, 2, \ldots.., n)$, there are n basic probability assignments $m_k(S_k)\,(k = 1, 2, \ldots.., n)$. Firstly, the combination of the first two data sources S_1 and S_2 can be obtained as:

$$m_1(\bar{S}_1) = \frac{\sum_{S_1 \cap S_2 = \bar{S}_1} m_1(S_1) \times m_2(S_2)}{1 - K_1}, \tag{16}$$

where K_1 is a normalized factor and represents a measure of conflict between two information sources, given by:

$$K_1 = \sum_{S_1 \cap S_2 = \phi} m_1(S_1) \times m_2(S_2). \tag{17}$$

When $K_1 = 1$, m does not exist and this means that the two information sources are in full contradiction. When $K_1 \neq 1$, the combination will be continued to fuse the next piece of evidence and the rest can be summarized as follows:

$$m_{n-1}(\bar{S}_{n-1}) = \frac{\sum_{\bar{S}_{n-2} \cap S_n = \bar{S}_{n-1}} m_{n-2}(\bar{S}_{n-2}) \times m_n(S_n)}{1 - \sum_{\bar{S}_{n-2} \cap S_n = \phi} m_{n-2}(\bar{S}_{n-2}) \times m_n(S_n)}. \tag{18}$$

In this study, the multi-scale TEO vector is considered as a basis for the evaluation of the local decision. In this study the basic probability assignment is defined as follows:

$$m_k(S_k) = \left(\frac{E_\sigma(i)}{\sum_{j=1}^{N} E_\sigma(j)} \right)_{i=1,\ldots,N} \tag{19}$$

It represents the local damage probability associated with each source, S_k, at each node, i, of the structure. m_k is an N-dimensional vector containing the damage probability at scale σ. The basic probability assignments can be combined through the theory of evidence and finally, the maximum component of the vector in Eq. (18) will indicate the damage location, which is called the improved-ULS index in the following.

It should be noted that the traditional ULS curvature change indicator illustrated in Eq. (7) needs the information of intact structure as baseline, while the improved ULS curvature depends only on the damaged structure. Based on the impacting force and the corresponding accelerometer response, the damaged structural flexibility is estimated and the ULS curves are calculated to serve as the input signal for the subsequent data fusion. Throughout the whole process, it is not required to consider the structural mass and intact structural information, which makes it more practical in real civil engineering.

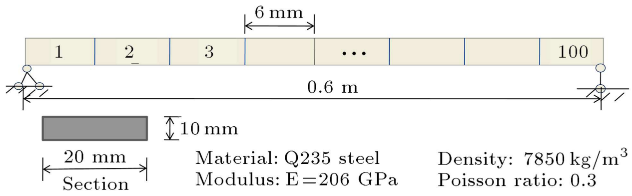

Figure 2. Simply supported steel beam model.

3. Numerical example

As shown in Figure 2, a simply supported steel beam model is used to study validity of the proposed method. The beam has a length of 0.6 m, which is divided into 100 elements. The material is Q235 steel with the elasticity of modulus of 206 GPa and unit weight of 7854 kg/m^3. The numerical model is simulated in SAP2000 software and a Rayleigh damping matrix is adopted. Three different levels of white noises are added to the response data to act as the observation noise.

Five damage patterns are considered:

- **Case 1.** Single damage scenario for 10% stiffness loss at the 60th element with 1% noise;
- **Case 2.** Single damage scenario for 10% stiffness loss at the 60th element with 2% noise;
- **Case 3.** Single damage scenario for 10% stiffness loss at the 60th element with 5% noise;
- **Case 4.** Multiple damage scenarios for 20% and 10% stiffness losses at the 30th and 70th elements with 1% noise; and
- **Case 5.** Multiple damage scenarios for 20% and 10% stiffness losses at the 30th and 70th elements with 2% noise.

The damage is simulated by reducing the width of the flange and details are illustrated in Table 1. Impacting forces are applied to the 30th and 60th nodes as excitation.

We take Case 1 as an example to illustrate the superiority of the proposed method. By performing an impact test on the beam, the corresponding accelerometer responses are recorded. Based on the impacting

Table 1. Damage cases used in the numerical model.

Case	Damage pattern	Damage location	Damage degree	Noise degree
Case 1	Single	60	10%	1%
Case 2	Single	60	10%	2%
Case 3	Single	60	10%	5%
Case 4	Multiple	30+70	20%+10%	1%
Case 5	Multiple	30+70	20%+10%	2%

force and accelerometer responses, the modal flexibility can be estimated by CMIF method, as plotted in Figure 3(a). To verify accuracy of the estimated modal flexibility, the static deflection measured by the corresponding static test is plotted to be compared with the displacement predicted from the flexibility. The static test is performed by placing 4 static forces with the magnitude of 100 kN on nodes 30, 60, and 90. The result is shown in Figure 3(b), and it can be seen that the predicted displacement has good agreement with the measured displacement, which demonstrates the accuracy of the identified flexibility.

Based on the identified flexibility, the Uniform Load Surface (ULS) is calculated by using the flexibility matrix to multiply the uniform force. Then, the ULS curvature can be obtained from Eq. (8). The ULS curvature in a noise-free environment is plotted in Figure 4(a) and in a 1% noisy environment is plotted in Figure 4(b). From the comparison, it can be found that a peak appears in the damage location by using the pure data, while the damage signature will be obscured in the noisy environment, even at a low noise level. Thus, we can conclude that the ULS curvature fails to identify the damage location unless the response data is pure. Obviously, this is impossible in real civil engineering testing.

Taking the ULS curve as an input signal, the multi-scale filtering approach is conducted according to Eq. (10) and the multi-scale space is constructed as shown in Figure 5(a). It can be seen that the filtered ULS curvature in each scale takes the shape of a flat curve and the damage features are insignificant. No obvious local extreme can be seen even in the small scale. To enhance the singularity of the filtered ULS curvature, the TEO values of ULS curvature are calculated in each scale according to Eq. (12). The obtained TEO-ULS curvatures are plotted in Figure 5(b). It can be seen that all the energy curves have local extreme around the damage location and they are invariant as the scale increases. However, it is difficult to locate the damage clearly based on only a single scale. Treating each scale as a different information source, Dempster-Shafer evidence rule is utilized to combine the evidences from scales and the basic probability assignments vector, $m_k(S_k)$, is obtained according to Eq. (19). In Case 1, 200 information sources have been accounted for, by $S_1 = \{E_{\sigma_1}\}, S_2 = \{E_{\sigma_2}\}, \ldots, S_{200} = \{E_{\sigma 200}\}$, and the scale parameter σ^2 is 2-4 with the interval of 0.01. Dempster-Shafer evidence rule is applied to the first two basic probability assignments to obtain the local decision vectors, $m_1(\bar{S}_1)$, and then, the final decisions vectors, $m_n(\bar{S}_n)$, are obtained according to

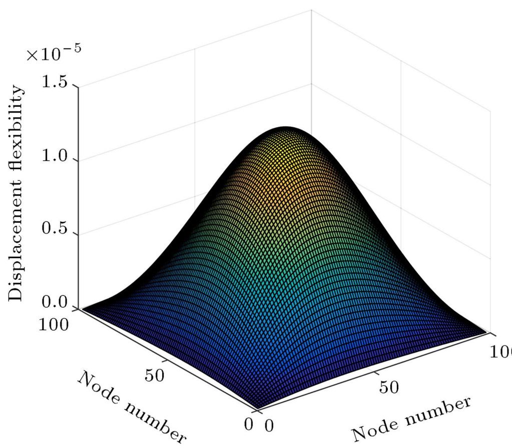

(a) Structural flexibility

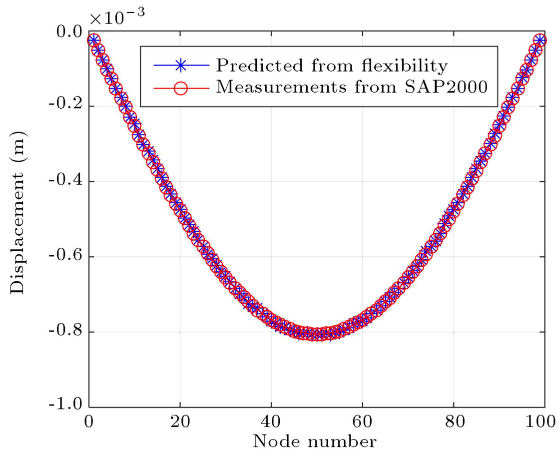

(b) Static displacement

Figure 3. Structural flexibility and predicted static displacement.

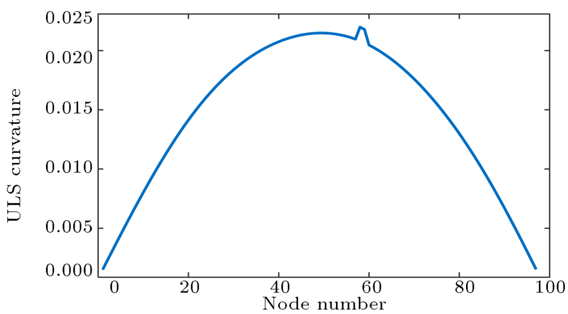

(a) In a noise free environment

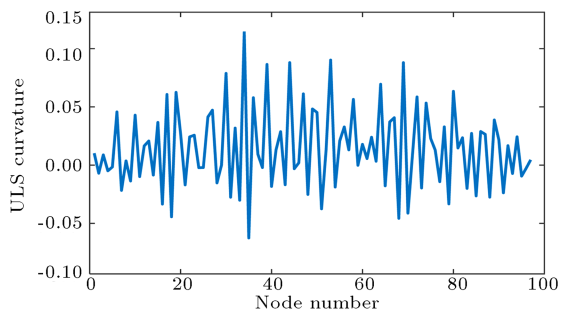

(b) In a 1% noise environment

Figure 4. Structural ULS curvature.

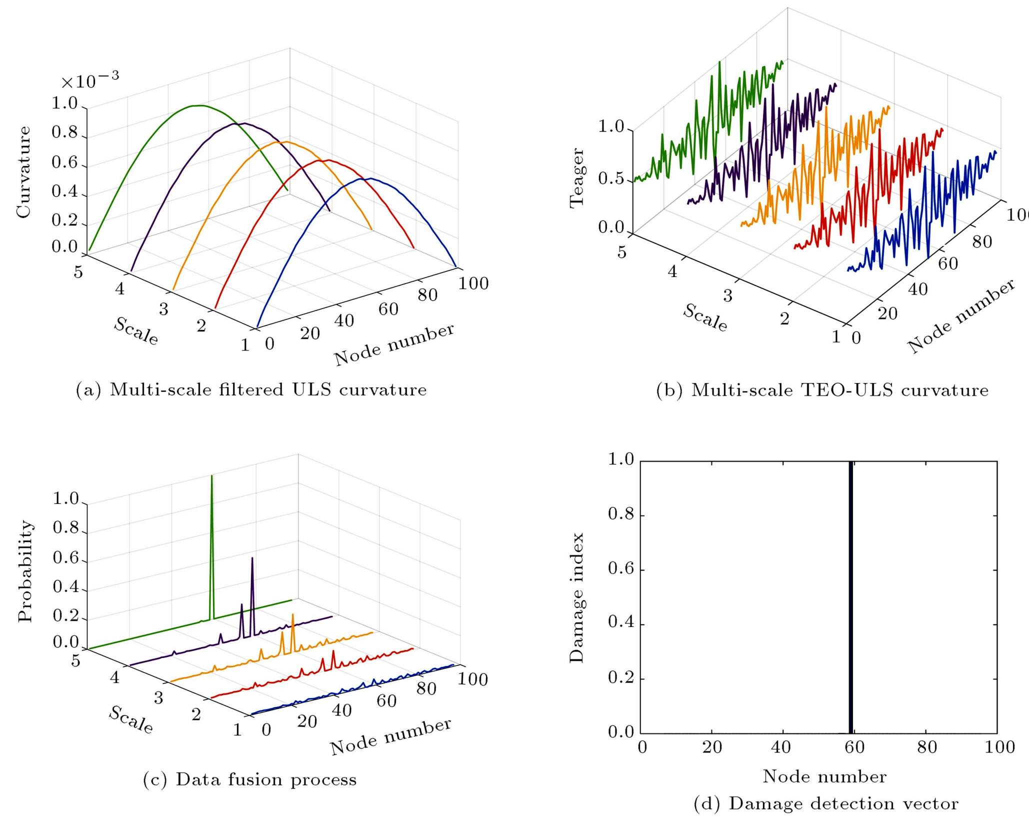

(a) Multi-scale filtered ULS curvature (b) Multi-scale TEO-ULS curvature

(c) Data fusion process (d) Damage detection vector

Figure 5. Data fusion technique to detect damage.

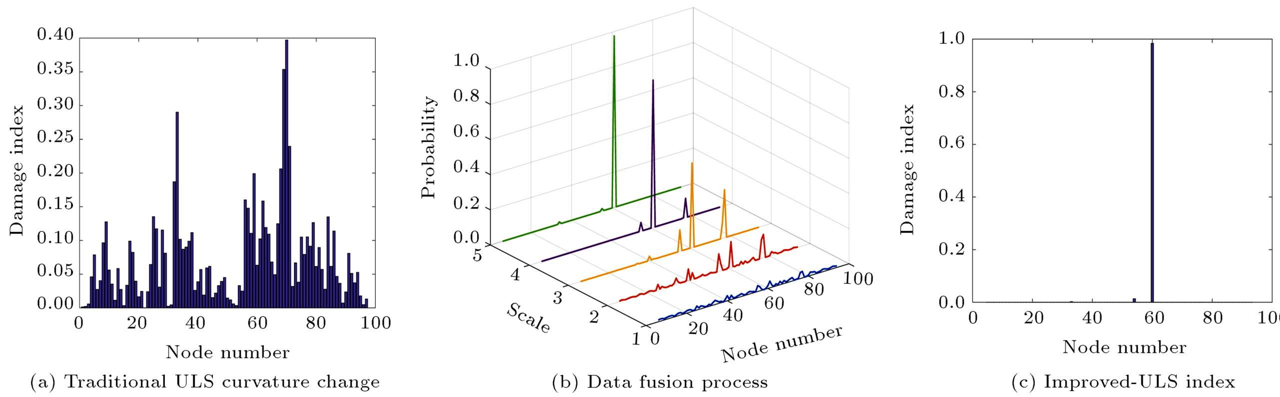

(a) Traditional ULS curvature change (b) Data fusion process (c) Improved-ULS index

Figure 6. Damage detection in Case 2.

Eq. (18). The fusion process has been plotted in Figure 5(c). It can be observed that the fluctuations are more violent and they totally conceal the damage feature at first. Then, with increase in the fusion, a peak appears around the damage location and the fluctuations are smoothed. The final decision vector is plotted in Figure 5(d). The highest value of probability provides clear evidence of damage locations, which demonstrates that the proposed method can locate the damage accurately.

Similar procedures are adopted for the other 4 cases to obtain the corresponding ULS curves. To validate the superiority of the proposed method, the traditional ULS curvature changes have been calculated according to Eq. (7) for comparison. The results are plotted in Figures 6(a), 7(a), 8(a), and 9(a) for the 4 damage cases. In addition, the proposed hybrid method is conducted and the fusion procedure is plotted in Figures 6(b), 7(b), 8(b), and 9(b). The final decision vector is plotted in Figures 6(c), 7(c), 8(c), and 9(c). By comparison, it can be found that the hybrid method performs better than the traditional ULS curvature change method, because the improved-ULS index can accurately locate the damage and has robustness to noise.

The traditional ULS curvature method fails to

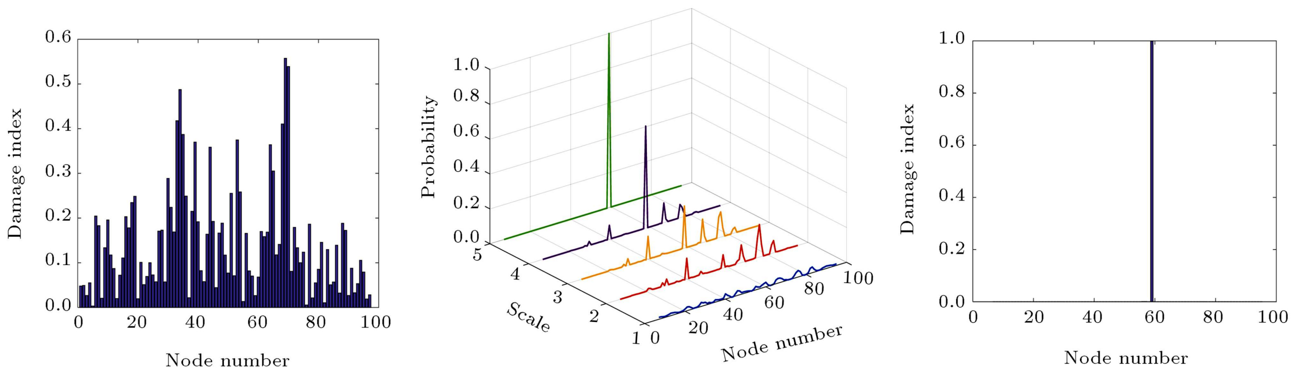

(a) Traditional ULS curvature change (b) Data fusion process (c) Improved-ULS index

Figure 7. Damage detection in Case 3.

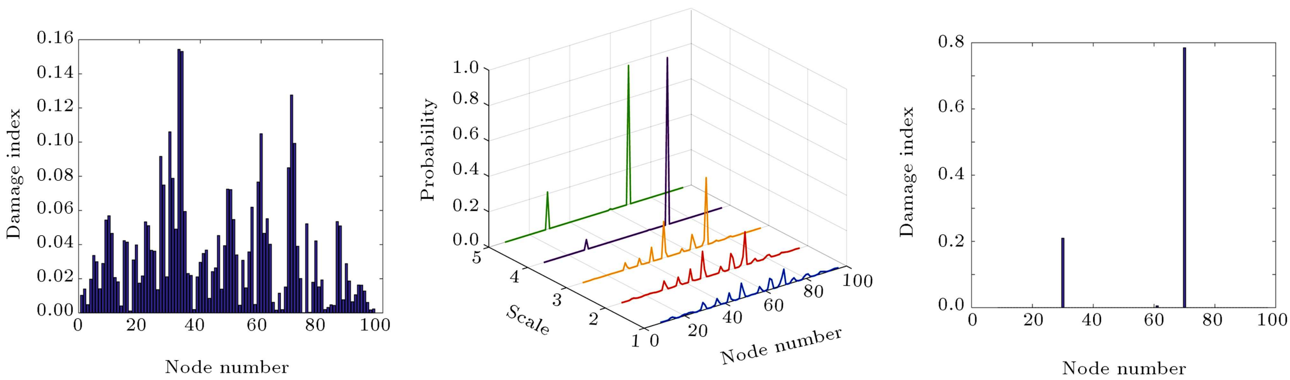

(a) Traditional ULS curvature change (b) Data fusion process (c) Improved-ULS index

Figure 8. Damage detection in Case 4.

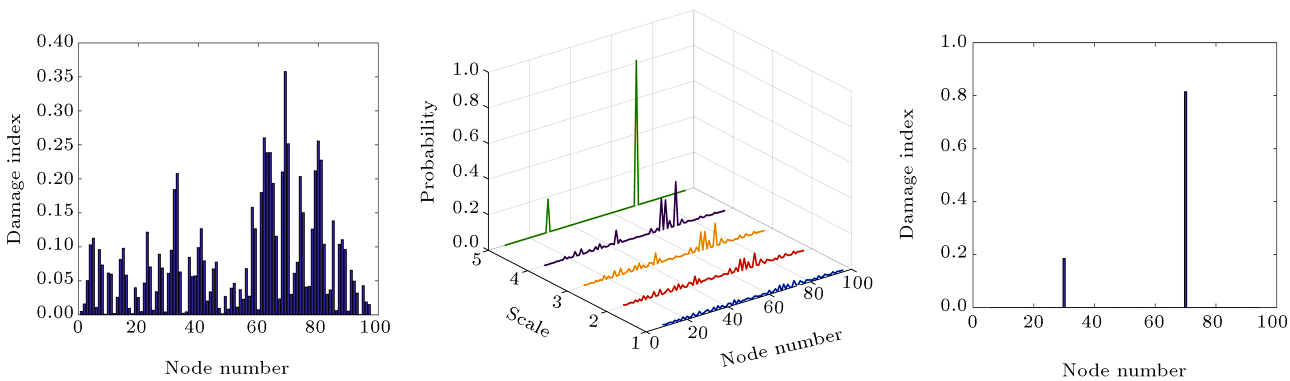

(a) Traditional ULS curvature change (b) Data fusion process (c) Improved-ULS index

Figure 9. Damage detection in Case 5.

detect damage with a low level of noise and the intact structure information is needed. On the other hand, the improved ULS curvature method only depends on the output response and utilizes the multi-scale Gaussian kernel function to filter ULS curves; then, it combines the basic probability assignments to obtain different information sources. Finally, the Dempster's rule is applied for obtaining the last decision vectors. Among the resultant figures, it can be seen that the improved ULS curvature method has the capacity to detect single damage with 5% noise and detect multiple damages with 2% noise. The damages are all obscured by noise if traditional ULS curvature method is used.

4. Experimental verification through a steel beam

In Section 3, the applicability of the proposed method was demonstrated by a numerical example. This section is devoted to verifying the robustness of the hybrid method by an experimental study of a simply supported I-section steel beam. The beam had a length of 5.76 m and its two ends were oriented on steel pedestals by clips. It was divided into 17 elements, which were continuously labeled from one end to the other. The configuration is illustrated in Figure 10. Sixteen accelerometers were placed on nodes from 1 to 16 and the NI PXIe-1082 data acquisition system was used for accelerometer measurements. The sampling of the measurement data was set to 0.001 s. In addition to the impact test, a static test was performed by placing 3 steel blocks with a mass of 91.8 kg on node 9 to measure the static displacement. Eight dial gauges were placed under the nodes 2, 4, 6, 8, 10, 12, 14, and 16 for displacement measurement. Two damage cases were considered:

- **Case 1.** Single damage scenario for 10% stiffness loss at the 7th element;
- **Case 2.** Multiple damages scenario for 10% and 15% stiffness losses at the 7th and 10th elements, respectively.

The damage was simulated by reducing the width of the flange.

The impacting force and acceleration response measured during the impact test were processed for displacement FRFs estimation and flexibility identification. By performing an impact test on the beam, the corresponding acceleration responses were recorded. The applied impacting force and acceleration responses are plotted in Figure 11(a) and (b). Displacement FRFs were estimated during the impact and, according to Eq. (1), the singular-value decomposition was applied to the estimated displacement FRFs to obtain the singular matrix, which is plotted in Figure 11(c). In the figure, 5 curves are plotted, because 5 nodes were impacted during the test. Four peaks in the spectral line represent the 4 modes that were identified. The natural frequencies in the first 4 modes were identified to be 15.1 Hz, 61.2 Hz, 129.4 Hz, and 230.78 Hz. The corresponding damping ratios were identified to be 0.083%, 0.08%, 0.51%, and 0.71%, respectively. The modal scaling factors can be obtained by Eq. (3). Thus, based on the identified basic modal parameters, the structural flexibility can be estimated by Eq. (5). Figure 11(d) plots the identified flexibility matrix, which has the dimensions of 16 by 16, because the simple supported beam had 16 nodes, as described above. To verify the accuracy of the estimated flexibility, the static displacement measured by the corresponding static test is plotted for comparison (Figure 11(e)). It can be seen that the predicted displacement has good agreement with the measured displacement, which demonstrates the accuracy of the estimated flexibility.

Based on the identified flexibility, the Uniform Load Surface (ULS) values of the structure can be obtained by Eq. (6). They are considered as the input signal to be convoluted with the Gaussian kernel function to obtain the multi-scale filtered ULS curvature. The results are plotted in Figure 12(a); it can be observed that the filtered ULS curvature became smoother when the scale increased. To enhance the singularity of the multi-scale ULS curvatures, the corresponding TEO values have been calculated by Eq. (12) and plotted in Figure 12(b). In the figure, it can be seen that the location of the local extreme emerging around the damage location (node 8) was invariant as the scale increased. Finally, different TEO values in different scales, which are considered as different information sources, are fused according to Eq. (18). The fusion process, as illustrated in Figure 12(c), combines the multi-scale TEO in different scales to get a joint support contribution, which is plotted in Figure 12(d). The highest part of this vector indicates the damage location.

Similar processes were applied to Case 2. When the impacting test and static test were completed on Case 1, the flange of the element near node 12 was cut to simulate multiple damages. Then, the impacting test of the simple supported beam was performed again. The impacting force and the corresponding accelerometer were recorded to estimate the displacement FRFs and flexibility, which are plotted on Figure 13(a). The

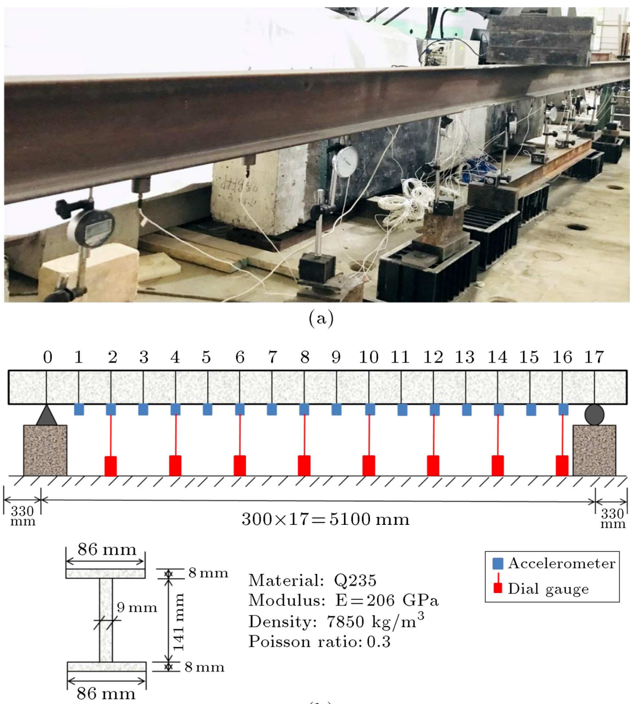

Figure 10. Illustration of the impact test: (a) Experiment layout and (b) configuration of the beam.

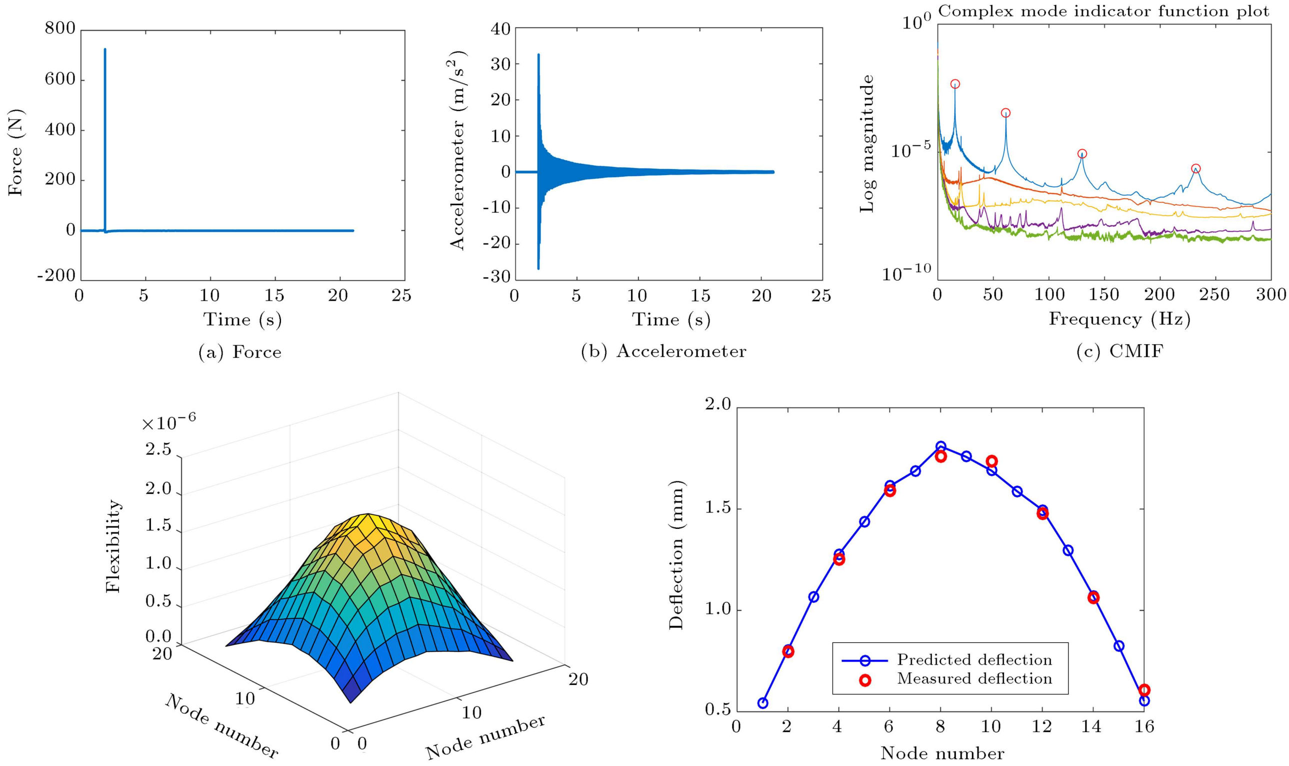

(a) Force (b) Accelerometer (c) CMIF

(d) Flexibility (e) Deflection

Figure 11. Flexibility identification process.

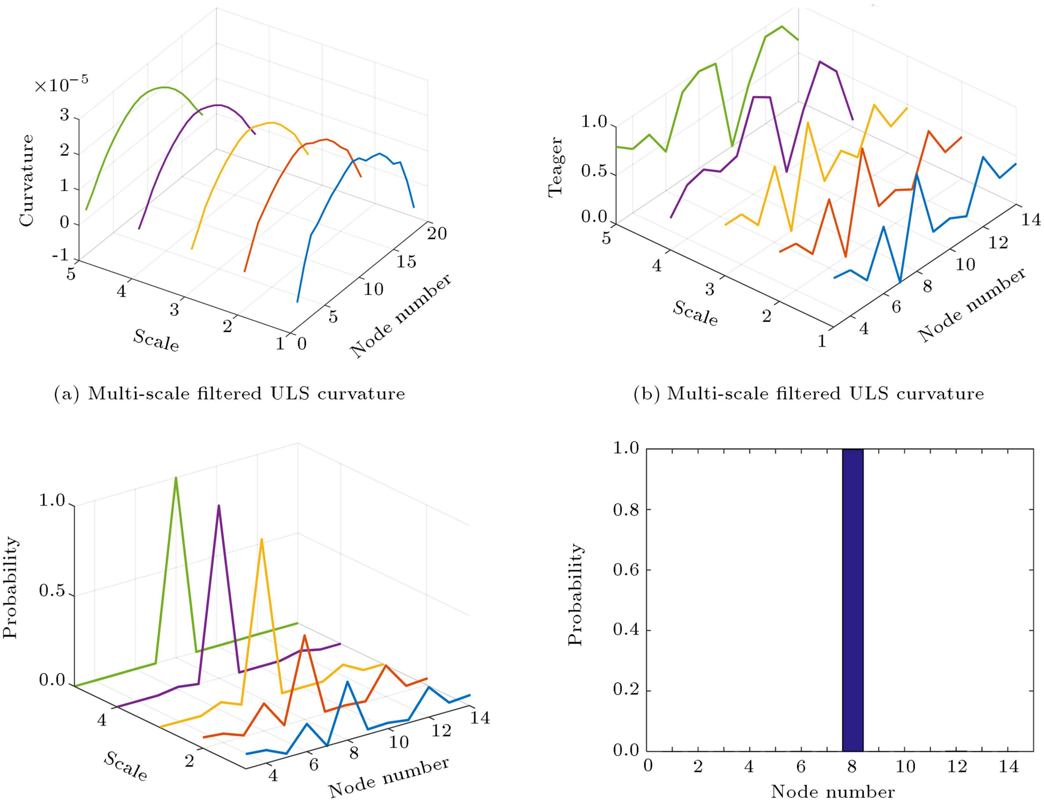

(a) Multi-scale filtered ULS curvature (b) Multi-scale filtered ULS curvature

(c) Data fusion process (d) Damage detection index

Figure 12. Experiment: damage detection in Case 1.

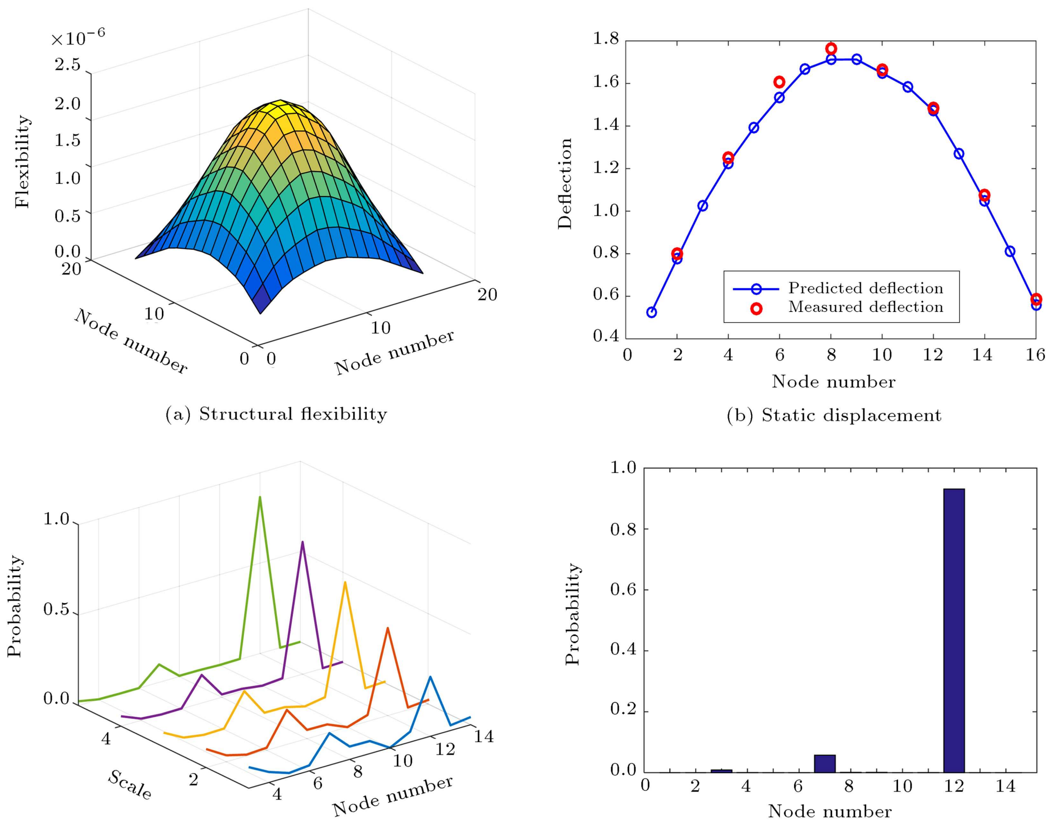

(a) Structural flexibility (b) Static displacement

(c) Data fusion process (d) Damage detection index

Figure 13. Experiment: damage detection in Case 2.

estimated flexibility is useful for structural performance evaluation and it can predict the structural displacement under static test. Figure 13(b) plots the predicted displacement when a block with the mass of 98.6 kg is placed on node 9. The measured displacement by dial gauges, seen as the theoretical value, is also plotted in Figure 13(b) for comparison. It is seen that the predicted displacement by modal flexibility agrees well with the measurements by dial gauge, which demonstrates the accuracy of the identified flexibility. The ULS curves were calculated and multi-scale convolution was utilized to obtain the multi-scale ULS curvature. Using Eq. (12), the multi-scale TEO vector was calculated to enhance local singularity. Finally, the Dempster-Shafer evidence theory was utilized to locate the damage by combining the information on all scales in order to obtain a reasonable result. The process is illustrated in Figure 13(c) and the final damage detection result is shown in Figure 13(d). It can be seen that the proposed method can accurately locate multiple damages in a noisy environment.

5. Conclusions

This study presents a novel hybrid method for damage detection in beams structures. The method was accomplished by a multi-scale analysis of the ULS curves, which were calculated from the estimated flexibility, to decrease the interference of the measurement noise. The Teager Energy Operator (TEO) was applied to each scale in order to enhance local singularity due to damage. Dempster-Shafer evidence theory was adopted to combine all scale information for amplifying the damage characteristics. Both numerical and experimental examples were utilized to verify robustness and effectiveness of the proposed method for damage detection in a noisy environment. Not only the structural mass, but also the intact structural flexibility serving as baseline was absent during the detection process, which provided the proposed method with a great application potential in damage detection in beams structure.

Acknowledgments

The research presented was financially supported by the National Key R&D Program of China (No.: 2018YFC0705601), Jiangsu Distinguished Young Scholars Fund (No.: BK20160002), and National Science Foundation of China (Grant No.: 51578139, 51608110).

References

1. Kaveh, A. and Zolghadr, A. "An improved charged system search for structural damage identification in beams and frames using changes in natural frequencies", *Int. J. of Optim. Civil. Eng.*, **3**(2), pp. 321-340 (2012).

2. Kaveh, A. and Zolghadr, A. "An improved CSS for damage detection of truss structures using changes in natural frequencies", *Adv Eng Softw*, **80**, pp. 93-100 (2015).

3. Cimellaro, G.P., Pianta, S., and Destefano, A. "Output-only modal identification of ancient L'Aquila city hall and civic tower", *ASCE J Struct Eng.*, **138**(4), pp. 481-491 (2012).

4. Zhang, J., Prader, J., Moon, F., et al. "Experimental vibration analysis for structural identification of a long span suspension bridge", *ASCE J Eng Mech.*, **139**(6), pp. 748-759 (2013).

5. Kaveh, A. and Maniat, A. "Damage detection based on MCSS and PSO using modal data", *Smart Structures and Systems*, **5**(15), pp. 1253-1270 (2015).

6. Kaveh, A. and Zolghadr, A. "A guided modal strain energy based approach for structural damage identification using tug of war optimization algorithm", *ASCE, J Comput Civil Eng.*, **31**(4), pp. 1-12 (2017). DOI:04017016

7. Kaveh, A., Vaez, S.R. Hoseini, and Hosseini, P. "Enhanced vibrating particle system algorithm for damage identification of truss structure", *Sci Iran*, **26**(1), pp. 246-256 (2019).

8. Zimmerman, D.C. and Kaouk, M. "Structural damage detection using a minimum rank update theory", *J Vib Acoust*, **116**, pp. 222-231 (1994).

9. Lu, Q., Ren, G., and Zhao, Y. "Multiple damage location with flexibility curvature and relative frequency change for beam structures", *J Sound Vib*, **253**(5), pp. 1101-1114 (2002).

10. Grande, E. and Imbimbo, M. "A multi-stage approach for damage detection in structural systems based on flexibility", *Mech Syst Signal Process*, **76-77**, pp. 455-475 (2016).

11. Zhang, Z. and Aktan, A.E. "Application of modal flexibility and its derivatives in structural identification", *Res Nondestruct Eval*, **10**, pp. 43-61 (1998).

12. Wang, J. and Qiao, P. "Improved damage detection for beam-type structures using a uniform load surface", *Struct Health Monit*, **6**, pp. 99-112 (2007).

13. Bernal, D. and Gunes, B. "Flexibility based approach for damage characterization: benchmark application", *J Eng Mech*, **130**, pp. 61-70 (2004).

14. Yan, W.J. and Ren, W.X. "Closed-form modal flexibility sensitivity and its application to structural damage detection without modal truncation error", *J Vib Control*, **20**(12), pp. 1816-1830 (2014).

15. Zhang, J., Xu, J.C., Guo, S.L., et al. "Flexibility-based structural damage detection with unknown mass for IASC-ASCE benchmark studies", *Eng Struct*, **48**, pp. 486-496 (2013).

16. Pandey, A.K. and Biswas, M. "Damage detection in structure using changes in flexibility", *J. Sound Vib*, **169**(1), pp. 3-17 (1994).

17. Hosseinzadeh, A.Z., Amiri, G.G., and Razzaghi, S.A.S., et al. "Structural damage detection using sparse sensors installation by optimization procedure based on the modal flexibility matrix", *J Sound Vib*, **381**, pp. 65-82 (2016).

18. Cheng, Y.Y., Zhao, C.Y., and Zhang, J. "Application of a novel long-gauge fiber bragg grating sensor for corrosion detection via a two-level strategy", *Sensors*, **19**(4), 954, pp. 1-18 (2019). DOI: 10.3390/s19040954

19. Sazonov, E. and Klinkhachorn, P. "Optimal spatial sampling interval for damage detection by curvature or strain energy mode shapes", *J. Sound Vib*, **285**, pp. 783-801 (2005).

20. Cao, M.S. and Qiao, P.Z. "Novel Laplacian scheme and multiresolution modal curvatures for structural damage identification", *Mech. Syst. Signal Process*, **23**, pp. 1223-1242 (2009).

21. Chandrashekhar, M. and Ganguli, R. "Damage assessment of structures with uncertainty by using mode shape curvatures and fuzzy logic", *J Sound Vib.*, **326**, pp. 939-957 (2009).

22. Cao, M.S., Radzienski, M., and Xu, W., et al. "Identification of multiple damage in beams based on robust curvature mode shapes", *Mech. Syst. Signal Process*, **46**, pp. 468-480 (2014).

23. Guo, H. "Structural damage detection using information fusion technique", *Mech. Syst. Signal Process*, **20**(5), pp. 1173-1188 (2006).

24. Grande, E. and Imbimbo, M. "A multi-stage approach for damage detection of linear system based on modal strain energy", *J. Civil Struct. Health Mon*, **4**, pp. 107-118 (2014).

25. Guo, T. and Xu, Z.L. "Data fusion of multi-scale representations for structural damage detection", *Mech. Syst. Signal Process*, **98**, pp. 1020-1033 (2018).

26. Peeters, B., Van der Auweraer, H., Guillaume, P., et al. "The PolyMAX frequency domain method: a new standard for modal parameter estimation", *Shock Vib.*, **11**(3-4), pp. 395-409 (2004).

27. Catbas, F.N., Brown, D.L., and Aktan, A.E. "Use of modal flexibility for damage detection and condition

assessment: case studies and demonstrations on large structures", *J Struct Eng.*, **132**(11), pp. 1699-1712 (2006).

28. Reynders, E. and Roeck, G.D. "Referenced-based combined deterministic-stochastic subspace identification for experimental and operational modal analysis", *Mech Syst Signal Process*, **22**(22), pp. 617-637 (2006).

29. Teager, H.M. and Teager S.M., *A Phenomenological Model for Vowel Production in the Cocal Tract*, College-Hill Press, San Diego (1983).

30. Kaiser, J.F. "On a simple algorithm to calculate the energy of a signal", in *IEEE Proceeding, ICASSP-90*, pp. 381-384 (1990).

31. Shafer, G., *A Mathematical Theory of Evidence*, Princeton University Press, Princeton, NJ (1976).

Biographies

Yuyao Cheng was born in 1989 in Anhui, China. Now, she is a PhD candidate in the School of Civil Engineering at Southeast University. Her research interests include structural damage detection, vibration testing, and the application of optical fiber sensing technology to structural health monitoring.

Chenyang Zhao was born in 1994 in Henan, China. Now, he is an MSc student in the School of Civil Engineering at Southeast University. His research focuses on structural damage detection based on the optical fiber sensing technology.

Jian Zhang was born in 1977 in Henan, China. He received his PhD degree from Kyoto University. Now, he is a Professor in the School of Civil Engineering at Southeast University and the director of Jiangsu Key Laboratory of Engineering Mechanics. His research mainly includes non-contact measurements, smart sensing, and vibration testing of large civil engineering structures.